

# Multipole Amplitudes of Pion Photoproduction on Nucleons up to $2 \text{ GeV}$ within Dispersion Relations and Unitary Isobar Model

I.G.Aznauryan

*Yerevan Physics Institute, Alikhanian Brothers St.2, Yerevan, 375036 Armenia*

(e-mail addresses: aznaury@jlab.org, aznaur@jerewan1.yerphi.am)

## Abstract

Two approaches for analysis of pion photo- and electroproduction on nucleons in the resonance energy region are checked at  $Q^2 = 0$  using the results of GWU(VPI) partial-wave analysis of photoproduction data. The approaches are based on dispersion relations and unitary isobar model. Within dispersion relations good description of photoproduction multipoles is obtained up to  $W = 1.8 \text{ GeV}$ . Within unitary isobar model, modified with increasing energy by incorporation of Regge poles, and with unified Breit-Wigner parametrization of resonance contributions, good description of photoproduction multipoles is obtained up to  $W = 2 \text{ GeV}$ .

PACS numbers: 13.60.Le, 14.20.Gk, 11.55.Fv, 11.80.Et

## 1 Introduction

It is known that dispersion relations (DR) and the unitary isobar model (UIM) constructed on the basis of effective Lagrangian approach in Ref. [1] are widely used for analysis of pion photo-and electroproduction data and for extraction from these data

information on  $\gamma^* N \rightarrow N^*$  vertices. In this paper our goal is to check these approaches at  $Q^2 = 0$  using the results of GWU(VPI) partial-wave analysis of pion photoproduction made from threshold to  $W = 2 \text{ GeV}$  (Ref. [2, 3] and SAID program). In the case of dispersion relations the main goal is to find the energy region of applicability of DR, because with increasing energy the utilization of DR is connected with the following problems: (a) at large angles the important  $P_{33}(1232)$  resonance contribution requires in the integrands of DR extrapolation to very large  $x = \cos\theta$  and becomes arbitrary, (b) the unknown contribution of resonances with large masses ( $M > 2 \text{ GeV}$ ) can become important, (c) the contribution of the Regge region ( $W > 2.5 \text{ GeV}$ ) can also become important. From the results of this paper it follows, that the role of these effects is insignificant up to  $W = 1.8 \text{ GeV}$ , and DR can be reliably used in this energy region.

In the case of the UIM our goal is to find adequate description of the resonance and background contributions in order to extend this model to  $W = 2 \text{ GeV}$ . It is known that the background of the UIM which consists of the minimal number of diagrams (the nucleon exchanges in the  $s$ - and  $u$ -channels and the  $t$ -channel  $\pi$ ,  $\rho$  and  $\omega$  exchanges) is motivated only at the threshold (Refs. [4, 5]) and in the first resonance region (Refs. [1, 6] and references therein). As it will be argued in Section 3, the extension of this background above first resonance region can not be satisfactory. Moreover, continued to  $2 \text{ GeV}$  and higher the background of Ref. [1] strongly contradicts experimental data. We will modify the UIM in such a way that with increasing energy the amplitudes of the model will transform into the amplitudes in the Regge pole regime which starts practically at  $W = 2.5 \text{ GeV}$ . We will demonstrate that incorporation of Regge poles into the background with increasing energy results in good description of GWU(VPI) photoproduction multipole amplitudes in the resonance energy region up to  $W = 2 \text{ GeV}$ . This description will be obtained using standard Breit-Wigner parametrization for the resonance contributions suggested in Ref. [7]. Only for the multipoles  $M_{1+}^{3/2}$ ,  $E_{1+}^{3/2}$  corresponding to the  $P_{33}(1232)$  resonance a slight modification will be made in order to satisfy the Watson theorem ([8]). Let us note that in order to reproduce photoproduction multipole amplitudes in the UIM of Ref. [1] complicated parametrization of resonance contributions

has been used. Such complication is caused by the fact that above first resonance region background contributions into some multipole amplitudes in Ref. [1] become too large, and in order to compensate them resonance contributions have been strongly deformed.

In Section 2 we will present our results obtained within dispersion relations. Firstly, in Sect. 2.1 we will present the results for multipole amplitudes  $M_{1+}^{3/2}$ ,  $E_{1+}^{3/2}$  which correspond to the  $P_{33}(1232)$  resonance. It will be shown, that DR for  $M_{1+}^{3/2}$ ,  $E_{1+}^{3/2}$  can be transformed into singular integral equations. These multipoles will be found via solutions of these equations. Further, in Sect. 2.2 imaginary parts of the contributions corresponding to other resonances will be found using the results of GWU(VPI) analysis and assuming Breit-Wigner parametrization of resonance contributions. We will find also nonresonance contributions into imaginary parts of  $E_{0+}^{(0,1/2,3/2)}$ ,  $M_{1-}^{(3/2)}$ ,  $M_{1+}^{(0,1/2)}$  and  $E_{1+}^{(0,1/2)}$  which are not small at small energies due to large  $\pi N$  phases  $\delta_{0+}^{1/2,3/2}$ ,  $\delta_{1-}^{3/2}$  and  $\delta_{1+}^{1/2}$ . These contributions will be found using DR and the Watson theorem. Finally, in Sect. 2.3 using DR, real parts of the multipole amplitudes will be found. In this Section the contribution of the multipole  $M_{1+}^{(3/2)}$  corresponding to the  $P_{33}(1232)$  resonance into DR for other multipoles will be investigated, and it will be shown that at  $W > 1.8 \text{ GeV}$  there is significant arbitrariness in the real parts of some multipole amplitudes connected with this contribution. The dispersion integrals over high energy region will be also estimated in Sect. 2.3, and it will be shown that the role of these integrals in the resonance energy region is insignificant.

In Section 3 we will discuss and present the modified UIM and will present the results obtained within this model. Conclusions will be made in Section 4.

## 2 Dispersion relations

We use fixed- $t$  dispersion relations for invariant amplitudes. Real parts of multipole amplitudes we derive via expansion of obtained results over multipoles. The invariant amplitudes are chosen following the work [9] in accordance with the following definition

of the hadron electromagnetic current:

$$I^\mu = \bar{u}(p_2)\gamma_5 \left\{ \frac{B_1}{2} [\gamma^\mu(\gamma\tilde{k}) - (\gamma\tilde{k})\gamma^\mu] + 2P^\mu B_2 + 2\tilde{q}^\mu B_3 + 2\tilde{k}^\mu B_4 - \gamma^\mu B_5 + (\gamma\tilde{k})P^\mu B_6 + (\gamma\tilde{k})\tilde{k}^\mu B_7 + (\gamma\tilde{k})\tilde{q}^\mu B_8 \right\} u(p_1), \quad (1)$$

where  $\tilde{k}$ ,  $\tilde{q}$ ,  $p_1$ ,  $p_2$  are 4-momenta of virtual photon, pion, initial and final nucleons, respectively,  $P = \frac{1}{2}(p_1 + p_2)$ ,  $B_1, B_2, \dots, B_8$  are invariant amplitudes which are functions of the invariant variables  $s = (\tilde{k} + p_1)^2$ ,  $t = (\tilde{k} - \tilde{q})^2$ ,  $Q^2 \equiv -\tilde{k}^2$ .

The conservation of the hadron electromagnetic current leads to the relations:

$$\begin{aligned} 4Q^2 B_4 &= (s - u)B_2 - 2(t + Q^2 - m_\pi^2)B_3, \\ 2Q^2 B_7 &= -2B'_5 - (t + Q^2 - m_\pi^2)B_8, \end{aligned} \quad (2)$$

where  $B'_5 \equiv B_5 - \frac{1}{4}(s - u)B_6$ . So, only the six of the eight invariant amplitudes are independent. Let us choose as independent amplitudes following ones:  $B_1, B_2, B_3, B'_5, B_6, B_8$ . The relations between these amplitudes and the multipoles are given in Appendix A. For all amplitudes  $B_1^{(\pm,0)}, B_2^{(\pm,0)}, B_3^{(+,0)}, B'_5^{(\pm,0)}, B_6^{(\pm,0)}, B_8^{(\pm,0)}$ , except  $B_3^{(-)}$ , unsubtracted dispersion relations at fixed  $t$  can be written:

$$\begin{aligned} \text{Re } B_i^{(\pm,0)}(s, t, Q^2) = & R_i^{(v,s)}(Q^2) \left( \frac{1}{s - m_N^2} + \frac{\eta_i \eta^{(+,-,0)}}{u - m_N^2} \right) \\ & + \frac{P}{\pi} \int_{s_{thr}}^{\infty} \text{Im } B_i^{(\pm,0)}(s', t, Q^2) \left( \frac{1}{s' - s} + \frac{\eta_i \eta^{(+,-,0)}}{s' - u} \right) ds', \end{aligned} \quad (3)$$

where  $R_i^{(v,s)}(Q^2)$  are residues in the nucleon poles (they are given in Appendix B),  $\eta_1 = \eta_2 = \eta_6 = 1$ ,  $\eta_3 = \eta'_5 = \eta_8 = -1$ ,  $\eta^{(+)} = \eta^{(0)} = 1$ ,  $\eta^{(-)} = -1$ ,  $s_{thr} = (m_N + m_\pi)^2$ . For the amplitude  $B_3^{(-)}$  we take the subtraction point at an infinity. In this case using the current conservation conditions (2) we have

$$\begin{aligned} \text{Re } B_3^{(-)}(s, t, Q^2) = & R_3^{(v)}(Q^2) \left( \frac{1}{s - m_N^2} + \frac{1}{u - m_N^2} \right) - \frac{eg F_\pi(Q^2)}{4\pi t - m_\pi^2} \\ & + \frac{P}{\pi} \int_{s_{thr}}^{\infty} \text{Im } B_3^{(-)}(s', t, Q^2) \left( \frac{1}{s' - s} + \frac{1}{s' - u} - \frac{4}{s' - u'} \right) ds', \end{aligned} \quad (4)$$

where the Born term, in addition to the nucleon poles, includes also the pion exchange in the  $t$ -channel.

Amplitudes  $B^{(+)}$ ,  $B^{(-)}$  correspond to isovector photon and are related to the amplitudes with definite value of total isospin in the  $s$ -channel by:

$$B^{(+)} = \frac{1}{3}(B^{(1/2)} + 2B^{(3/2)}), \quad B^{(-)} = \frac{1}{3}(B^{(1/2)} - B^{(3/2)}), \quad (5)$$

amplitude  $B^{(0)}$  corresponds to isoscalar photon.

Amplitudes corresponding to definite reactions are:

$$\begin{aligned} B(\gamma + p \rightarrow p + \pi^0) &= B^{(+)} + B^{(0)}, \\ B(\gamma + n \rightarrow n + \pi^0) &= B^{(+)} - B^{(0)}, \\ B(\gamma + p \rightarrow n + \pi^+) &= 2^{1/2}(B^{(0)} + B^{(-)}), \\ B(\gamma + n \rightarrow p + \pi^-) &= 2^{1/2}(B^{(0)} - B^{(-)}). \end{aligned} \quad (6)$$

We will use also the following notations:

$${}_p B^{\frac{1}{2}} = B^{(0)} + \frac{1}{3}B^{(1/2)}, \quad {}_n B^{\frac{1}{2}} = B^{(0)} - \frac{1}{3}B^{(1/2)}. \quad (7)$$

where the subscript  $p$  ( $n$ ) denotes a proton (neutron) target.

## 2.1 $P_{33}(1232)$ resonance

Let us write dispersion relations for the multipole amplitudes  $M_{1+}^{3/2}/kq$ ,  $E_{1+}^{3/2}/kq$  in the form

$$M(W) = M^B(W) + \frac{1}{\pi} \int_{W_{thr}}^{W_{max}} \frac{ImM(W')}{W' - W - i\varepsilon} dW' + \frac{1}{\pi} \int_{W_{thr}}^{W_{max}} K(W, W') ImM(W') dW', \quad (8)$$

where  $M(W)$  denotes any of multipoles  $M_{1+}^{3/2}/kq$ ,  $E_{1+}^{3/2}/kq$ ,  $k$  and  $q$  are the photon and pion 3-momenta in the c.m.s.,  $M^B(W)$  is the contribution of the Born term into these multipoles,  $K(W, W')$  is a nonsingular kernel arising from the u-channel contribution into the dispersion integral and the nonsingular part of the s-channel contribution,  $W_{max} = 1.8 \text{ GeV}$ .

In the relations (8) the following assumptions are made:

(a) For each amplitude  $M_{1+}^{3/2}/kq$ ,  $E_{1+}^{3/2}/kq$  we neglect the contributions of other multipoles

into dispersion integrals. By our estimations they are small and do not affect our final results. These contributions are shown by thin dashed curves in Figs. 1a,b. It is seen that up to  $1.8 \text{ GeV}$  they are practically equal to 0 for  $M_{1+}^{3/2}$  and are very small for  $E_{1+}^{3/2}$ . (b) We neglect the integrals over ( $W_{max} = 1.8 \text{ GeV}, \infty$ ). In Figs. 1a,b we have presented the results of GWU(VPI) partial-wave analysis for  $M_{1+}^{3/2}$  and  $E_{1+}^{3/2}$  up to  $W = 2 \text{ GeV}$ . It is seen that at  $1.8 \text{ GeV} < W < 2 \text{ GeV}$ ,  $ImM_{1+}^{3/2}$  and  $ImE_{1+}^{3/2}$  are practically equal to 0. The integrals over ( $2 \text{ GeV}, \infty$ ) were estimated using the results of the Regge-pole analysis of high energy data made in Ref. [10]. These integrals turned out to be negligibly small.

Let us make one more assumption:

(c) We will use the Watson theorem from threshold to  $W = 1.8 \text{ GeV}$ , assuming that  $\delta_{1+}^{3/2}(W) \rightarrow \pi$ , i.e.  $ImM(W) \rightarrow 0$ , when  $W \rightarrow W_{max}$ . From the results of GWU(VPI) partial-wave analysis presented in Figs. 1a,b it is seen that this is reasonable assumption, taking into account that the  $\pi N$  amplitude  $h_{1+}^{3/2}(W)$  is elastic up to  $W = 1.45 \text{ GeV}$ , and at  $W = 1.45 \text{ GeV}$ ,  $\delta_{1+}^{3/2} = 157^\circ$  [11]. So, in all integration region we will take  $ImM(W) = h^*(W)M(W)$ .

With these assumptions the dispersion relations for  $M_{1+}^{3/2}, E_{1+}^{3/2}$  turn into singular integral equations (8), which at  $K(W, W') = 0$  have solutions in an analytical form ([12, 13]):

$$M_{K=0}(W) = M_{part, K=0}^B(W) + c_M M_{K=0}^{hom}(W), \quad (9)$$

where  $M_{part, K=0}^B(W)$  is the particular solutions of Eq. (8) generated by  $M^B$ :

$$M_{part, K=0}^B(W) = M^B(W) + \frac{1}{\pi} \frac{1}{D(W)} \int_{W_{thr}}^{W_{max}} \frac{D(W')h(W')M^B(W')}{W' - W - i\varepsilon} dW', \quad (10)$$

and

$$M_{K=0}^{hom}(W) = \frac{1}{D(W)} = \frac{W_{max}}{|W_{max} - W|} \exp \left[ \frac{W}{\pi} \int_{W_{thr}}^{W_{max}} \frac{\delta(W')}{W'(W' - W - i\varepsilon)} dW' \right] \quad (11)$$

is the solution of the homogeneous equation (8) with  $M^B = 0$ . It enters the solution (9) with an arbitrary weight, i.e. multiplied by an arbitrary constant  $c_M$ .

At  $K(W, W') \neq 0$  one can transform the singular integral equation (8) into nonsingular integral equation ([14]). The solution of this equation turned out to be very close to (9).

From Eqs. (9-11) it is seen that with given  $M^B(W)$ , the particular and homogeneous solutions of the integral equation (8) are determined only by the phase  $\delta_{1+}^{3/2}(W)$ . In our calculations, at  $W < 1.35 \text{ GeV}$ , this phase was taken in the form:

$$\sin^2 \delta_{1+}^{3/2} = \frac{(4.27q^3)^2}{(4.27q^3)^2 + (q_r^2 - q^2)^2[1 + 40q^2(q^2 - q_r^2) + 21.4q^2]^2}, \quad (12)$$

which is a slightly modified version of the corresponding formula from Ref. [15],  $q_r$  is the pion c.m.s. momentum at  $W = M$ . At  $1.35 \text{ GeV} < W < 1.8 \text{ GeV}$ , the phase was taken in the form:

$$\delta = \pi - [\pi - \delta(W = 1.35 \text{ GeV})] \left( \frac{q - q_2}{q_1 - q_2} \right)^2, \quad (13)$$

where  $q_1$  and  $q_2$  are the pion c.m.s. momenta, respectively, at  $W = 1.35 \text{ GeV}$  and  $W = 1.8 \text{ GeV}$ . Eqs. (12,13) reproduce with good accuracy the results of the GWU(VPI) analysis for  $\delta_{1+}^{3/2}(W)$  from threshold to  $W = 1.5 \text{ GeV}$ .

Our final results for  $M_{1+}^{3/2}$ ,  $E_{1+}^{3/2}$ , obtained by the formulas (9-13) via adjusting the only unknown parameters  $c_M$  and  $c_E$ , are presented in Figs. 1a,b. It is seen that there is good agreement with the GWU(VPI) results. In Fig. 1a we have presented also separately contributions of particular and homogeneous solutions into imaginary part of  $M_{1+}^{3/2}$ .

## 2.2 Imaginary parts of multipole amplitudes up to 2 GeV

In the resonance energy region imaginary parts of multipole amplitudes are determined mainly by the resonance contributions. These contributions for the resonances which are seen in the GWU(VPI) analysis at  $W < 2 \text{ GeV}$ , except  $P_{33}(1232)$ , we have found using Breit-Wigner parametrization given in Appendix C. Good description of the imaginary parts of multipole amplitudes was obtained with parameters in the Breit-Wigner formula presented in Table 1.

At small energies imaginary parts of the amplitudes  $E_{0+}^{(0,1/2,3/2)}$ ,  $M_{1-}^{(3/2)}$ ,  $M_{1+}^{(0,1/2)}$ ,  $E_{1+}^{(0,1/2)}$  contain also noticeable nonresonance contributions due to large  $\pi N$  phases  $\delta_{0+}^{1/2,3/2}$ ,

Resonance	$M, \text{ GeV}$	$\Gamma, \text{ GeV}$	$X$
$P_{11}(1440)$	1.45 (1.46)	0.3	0.3
$S_{11}(1535)$	1.52	0.11 (0.12)	0.5
$D_{13}(1520)$	1.51	0.12 (0.1)	0.1 (0.3)
$S_{11}(1650)$	1.65	0.08 (0.11)	0.5
$F_{15}(1680)$	1.68	0.13	0.2 (0.5)
$P_{13}(1720)$	1.8	0.38 (0.35)	0.5 (0.4)
$S_{31}(1620)$	1.61 (1.62)	0.14	0.5
$D_{33}(1700)$	1.65	0.25	0.22 (0.2)
$F_{37}(1950)$	1.92 (1.93)	0.3	0.5

Table 1: Parameters in the Breit-Wigner formula from Appendix C, found via description of imaginary parts of multipole amplitudes. In the parentheses the parameters found within UIM are presented in the cases when they differ from the parameters found in this Section.

$\delta_{1-}^{3/2} \delta_{1+}^{1/2}$ . Up to  $W = 1.3 \text{ GeV}$  these contributions were found using DR and the Watson theorem. At higher energies they were reduced to 0.

Our final results for the imaginary parts of the multipole amplitudes obtained in the way described in this Section are presented by dashed curves in Fig. 2.

### 2.3 Real parts of multipole amplitudes

Real parts of multipole amplitudes were found using dispersion relations (3,4). Let us present dispersion integrals in these relations in the form:

$$\int_{W_{thr}}^{\infty} = \int_{W_{thr}}^{2 \text{ GeV}} + \int_{2 \text{ GeV}}^{2.5 \text{ GeV}} + \int_{2.5 \text{ GeV}}^{\infty}. \quad (14)$$

Imaginary parts of the amplitudes in the first integral over resonance energy region from threshold to 2 GeV are known from the results of Sections 2.1 and 2.2. The only

uncertainty which can arise in this integral with increasing energy at large angles is connected with the contribution of the  $P_{33}(1232)$  resonance. This uncertainty is the result of the extrapolation of the  $P_{33}(1232)$  contribution in the integrands at large  $|t|$  to very large  $x' = \cos(\theta')$ . Such extrapolation with increasing  $x'$  becomes arbitrary. In addition, the contribution of the multipole  $M_{1+}^{3/2}$ , which is large by itself, sharply grows with increasing energy. This is demonstrated in Figs. 1b and 3 for the amplitudes  $E_{1+}^{3/2}$ ,  $E_{0+}^{1/2,3/2}$ ,  $M_{1-}^{1/2,3/2}$ . Let us note, that at  $W > 1.7 - 1.8 \text{ GeV}$  these amplitudes are much smaller than the  $P_{33}(1232)$  resonance contribution (see Figs. 2a-f), and therefore should be obtained as differences of two large contributions, one of which, the  $P_{33}(1232)$  contribution, contains arbitrariness. By this reason, with increasing energy we have significant arbitrariness in the real parts of some multipole amplitudes connected with the  $P_{33}(1232)$  resonance contribution.

Imaginary parts of the amplitudes in the integrals over high energy region from  $2.5 \text{ GeV}$  to  $\infty$  can be found using the results of Regge-pole analysis made in Ref. [10]. The way of construction of the amplitudes in Ref. [10] is described in Appendix D. This analysis is made in gauge-invariant form and in terms of invariant amplitudes. By this reason its results can be easily used for the calculation of high energy integrals in the dispersion relations (3,4). The role of these integrals turned out to be negligible in the real parts of multipoles in the I and II resonance regions and very small in the III and IV resonance regions.

Imaginary parts of the amplitudes in the integrals over intermediate energy region were calculated via interpolation of the imaginary parts of the amplitudes between the regions:  $W < 2 \text{ GeV}$  and  $W > 2.5 \text{ GeV}$ .

Our final results for real parts of the multipole amplitudes are presented in Fig. 2 by dashed-dotted curves. Let us note that in Fig. 2 all amplitudes, for which the GWU(VPI) analysis gives definite results, are presented. It is seen that the agreement with the GWU(VPI) results is satisfactory up to  $W = 1.8 \text{ GeV}$ . At higher energies in some multipoles noticeable deviations from the GWU(VPI) results arise. Most probably they are connected with the above discussed  $P_{33}(1232)$  resonance contribution. These

deviations strongly depend on the small changes of the magnitude and the shape of the multipole  $M_{1+}^{3/2}$  corresponding to the  $P_{33}(1232)$  resonance. In addition, when we approach  $W = 2 \text{ GeV}$ , the uncertainty connected with the unknown contribution of the resonances with  $M > 2 \text{ GeV}$  can become significant. By these reasons multipole amplitudes obtained by DR at  $W > 1.8 \text{ GeV}$  are not reliable, and we do not present them in Fig. 2.

### 3 Unitary isobar model

The unitary isobar model is based on the effective Lagrangian approach which was introduced in Refs. [4, 5] to reproduce low energy results of current algebra and PCAC. Within the approach of Refs. [4, 5] the pion photoproduction amplitudes consist of nucleon exchanges in the  $s$ - and  $u$ -channels and  $t$ -channel  $\pi$  exchange with pseudovector  $\pi NN$  constant and contact term presented in Appendix B. These contributions describe well the pion photoproduction on the nucleons at the threshold ( Ref. [5]).

Later the approach of Refs. [4, 5] was extended to the  $P_{33}(1232)$  resonance region in the number of works (see, for example, references in Refs. [1, 6]), and to the first, second and third resonance regions in the UIM [1]. Background of the UIM is constructed from the contributions of the nucleon exchanges in the  $s$ - and  $u$ -channels and  $t$ -channel  $\pi$  exchange with  $\pi NN$  constant which, being pure pseudovector at the threshold, with increasing energy transforms into pseudoscalar constant via the formula (B.2). In addition to these contributions, the background of the UIM [1] contains the  $t$ -channel  $\rho$  and  $\omega$ -exchanges, which are given in Appendix E. The background, constructed in this way, is unitarized for each multipole amplitude according to Ref. [16] in the  $K$ -matrix approximation:

$$\text{Unitarized}(M_{l\pm}, E_{l\pm}, S_{l\pm})_{\text{background}} = (M_{l\pm}, E_{l\pm}, S_{l\pm})_{\text{background}}(1 + ih_{\pm}^{\pi N}). \quad (15)$$

With increasing energy the contribution of this background into some multipole amplitudes becomes too large. This is demonstrated in the case of  $M_{1+}^{3/2}$  in Fig. 1d (dotted curve). In order to compensate these large background contributions, resonance contri-

butions in the UIM of Ref. [1] have been strongly deformed. Continued to the energies  $W > 2 \text{ GeV}$  the background of Ref. [1] strongly contradicts experimental data.

Extension of the effective Lagrangian approach above first resonance region with the minimal set of diagrams (the nucleon exchanges in the  $s$ - and  $u$ -channels and  $t$ -channel  $\pi$ ,  $\rho$  and  $\omega$ -exchanges) can not be satisfactory by the following reasons:

- (i) Restriction by the mesons with lowest masses in the  $t$ -channel exchanges is justified only at small energies, where  $t$  is small and, therefore, the propagators  $1/(t - m_{mes}^2)$  are determined by the meson masses. However, with increasing energy the range of  $t$  is increasing, and additional  $t$ -channel contributions corresponding to the mesons with higher masses should be taken into account.
- (ii) With increasing energy, starting with  $W = 1.3 \text{ GeV}$ , the contributions of inelastic channels into  $\pi N$  scattering become important (see, for example, Ref. [17]). This means that the diagrams corresponding to the production of other particles with subsequent rescattering, i.e.  $\gamma N \rightarrow \text{inel.} \rightarrow \pi N$ , should be taken into account.

So, in order to extent consistently effective Lagrangian approach above first resonance region, it is necessary to take into account a large amount of new diagrams.

From the other hand, it is known that with increasing energy regularization of different contributions occurs via multiple gluon exchanges between  $t$ -channel quarks, and all contributions are reduced to the restricted number of regularized  $t$ -channel exchanges. This picture, which is known as Regge-pole model, gives good description of exclusive reactions above  $W = 2.5 \text{ GeV}$  ( $E_\gamma = 3 \text{ GeV}$ ) at  $t < 3 \text{ GeV}^2$ . In the number of cases Regge-pole approach gives good description at smaller energies too.

By this reason we have modified the unitary isobar model in such a way, that it incorporates the results of the effective Lagrangian approach in the first resonance region and the Regge-pole behaviour of amplitudes at high energies. With this aim we have made the following modifications:

- (a) Background is constructed in the form:

$$Back = [N + \pi + \rho + \omega]_{UIM} \frac{1}{1 + (s - s_0)^2} + [\pi + \rho + \omega + b_1 + a_2]_{Regge} \frac{(s - s_0)^2}{1 + (s - s_0)^2}, \quad (16)$$

where the Regge-pole amplitudes are presented in Appendix D. They are taken from the analysis of high energy photoproduction data made in Ref. [10].

(b) Resonance contributions are parametrized in the standard Breit-Wigner form presented in Appednix C. With increasing energy these contributions tend to 0, and the amplitudes of the modified UIM are equal approximately to the Regge-pole amplitudes beginning with  $W = 2.5 \text{ GeV}$ .

Within the unitary isobar model modified in this way, good description of all multipole amplitudes with  $l \leq 3$  is obtained up to  $W = 2 \text{ GeV}$ , taking  $s_0 = 1.2 \text{ GeV}^2$ . The results obtained using  $\pi N$  amplitudes in the unitarization procedure (15) from the GWU(VPI) analysis (SAID program) are presented in Figs. 1b-d and 2 (bold solid curves). For comparison in Figs. 1b and 2 the results obtained with the same resonance contributions and with the background of the UIM of Ref. [1] are presented (thin solid curves). It is seen that for the multipoles  ${}_pM_{1-}^{1/2}$ ,  ${}_pM_{2-}^{1/2}$ ,  ${}_pE_{2-}^{1/2}$ ,  ${}_nE_{2-}^{1/2}$ ,  $E_{2-}^{3/2}$ ,  ${}_pE_{3-}^{1/2}$ ,  ${}_pM_{3-}^{1/2}$ ,  $M_{3+}^{3/2}$  they strongly contradict the GWU(VPI) results.

From Figs. 1b-d and 2a-i it is seen that for the multipole amplitudes with  $l = 0, 1$  the deviation between the results obtained with the modified and nonmodified backgrounds becomes to be seen at  $W > 1.3 \text{ GeV}$ , i.e. above first resonance region. For the multipoles with  $l = 2, 3$ , except  $E_{2+}^{3/2}$  (Fig. 2o), this deviation is noticeable already in the first resonance region. However, for large multipoles  ${}_pE_{2-}^{1/2}$ ,  ${}_nE_{2-}^{1/2}$ ,  $E_{2-}^{3/2}$  (Figs. 2l-n) the deviation does not exceed the errors of the GWU(VPI) data. For the multipoles  ${}_pM_{2-}^{1/2}$ ,  ${}_pE_{3-}^{1/2}$ ,  ${}_pM_{3-}^{1/2}$ ,  $M_{3+}^{3/2}$  (Figs. 2k,p-r) there is no results of partial-wave analyses below  $W = 1.3 \text{ GeV}$ , however, these multipoles are very small in this energy region. Moreover, with increasing energy the multipoles  ${}_pM_{2-}^{1/2}$ ,  ${}_pE_{3-}^{1/2}$ ,  ${}_pM_{3-}^{1/2}$ ,  $M_{3+}^{3/2}$  obtained with the modified background are in better agreement with the GWU(VPI) results.

Let us note that for the  $P_{33}(1232)$  resonance we have modified the Breit-Wigner parametrization given in Eq. (C.1), taking  $\Gamma_{total}$  in the form  $\Gamma_{total} = \Gamma_\pi \frac{M^2}{s}$ . This gives good description of the ratio of the imaginary and real parts of the amplitudes  $M_{1+}^{3/2}$ ,  $E_{1+}^{3/2}$ ,  $S_{1+}^{3/2}$  in accordance with the Watson theorem. Let us note that background contributions into these multipoles, unitarized via Eq. (15), satisfy the Watson theorem. In the case

of the amplitude  $M_{1+}^{3/2}$  which is known with great accuracy, the following modifications are also made:

- (a) At  $W < 1.3 \text{ GeV}$  the right part of the Eg. (C.1) is multiplied by the factor  $(W/M)^6$ .
- (b) At  $W > 1.3 \text{ GeV}$  the imaginary and real parts of the resonance contribution are multiplied by the factors  $I_{Im}$  and  $I_{Re}$ :

$$I_{Im} = \frac{(W/1.3)^{2.5}(1.3/M)^6}{1 + 2.4(s - 1.69)^{2.5}}, \quad I_{Re} = \frac{(W/1.3)^{3.5}(1.3/M)^6}{1 + 1.4(s - 1.69)^{2.5}}, \quad (17)$$

where  $W$  and  $M$  are in the  $\text{GeV}$  units. These are slight modifications. The obtained resonance contribution into  $M_{1+}^{3/2}$  is presented in Figs. 1c,d by dashed-dotted curves. It is seen that sum of this contribution and modified background contribution (dashed curves) describe well the GWU(VPI) data. With background of Ref. [1] (dotted curves), resonance contribution should be strongly deformed in order to describe the GWU(VPI) data.

With the above described modifications, we have obtained good description of the  $P_{33}(1232)$  resonance contribution at  $Q^2 \neq 0$  too. To demonstrate this in Fig. 4 the imaginary part of  $M_{1+}^{3/2}$  is presented at  $Q^2 = 0.9, 1.8, 2.8, 4 \text{ GeV}^2$  (solid curves). In this Figure  $Im M_{1+}^{3/2}$  obtained within DR via solution of the integral equation (8) is also presented (dashed curves). These results are obtained from the analysis of JLab data [18, 19]. It is seen that the amplitudes obtained within two approaches are in good agreement with each other. In order to compare the shape of the amplitude  $M_{1+}^{3/2}$  at  $Q^2 \neq 0$  with its shape at  $Q^2 = 0$ , we have presented in Fig. 4 the GWU(VPI) data with the normalizations corresponding to  $Q^2 = 0.9, 1.8, 2.8, 4 \text{ GeV}^2$ . It is seen that the shape of  $M_{1+}^{3/2}$  practically does not change with increasing  $Q^2$ .

## 4 Conclusion

We have obtained good description of real parts of all multipole amplitudes with  $l \leq 3$  up to  $W = 1.8 \text{ GeV}$  using fixed- $t$  dispersion relations. In Sec. 2.1 it is shown, that dispersion relations for multipole amplitudes  $M_{1+}^{3/2}, E_{1+}^{3/2}$  which correspond to the  $P_{33}(1232)$

resonance, can be transformed into singular integral equations. The real and imaginary parts of these multipoles were obtained via solution of these equations and are in good agreement with the GWU(VPI) results.

We have modified the unitary isobar model of Ref. [1] via incorporation of Regge poles with increasing energy and using unified Breit-Wigner parametrization of resonance contributions in the form proposed in Ref. [7]. Within this approach we have obtained good description of all photoproduction multipoles with  $l \leq 3$  up to  $W = 2 \text{ GeV}$ .

Both approaches can be continued to  $Q^2 \neq 0$ , and all formulas in this paper are presented in the form which allows to make this continuation. Therefore, both approaches can be used for analysis of data on pion electroproduction on nucleons and for extraction from these data information on  $Q^2$ -evolution of  $\gamma^* N \rightarrow N^*$  form factors. It is known, that this problem is very actual at present due to the experimental investigation of this reaction on high duty-factor electron accelerator at Jefferson Lab.

## Acknowledgments

I am thankful to V.D.Burkert, who has drawn my attention to the unitary isobar model. I am greatful to S.G.Stepanyan for his cooperation in writing codes for both approaches. I would like to thank V.I.Mokeev for very usefull discussions, to R.L.Crawford for discussions of the problems which can arise in dispersion relations with increasing energy and to I.I.Balitsky and N.Ya.Ivanov for discussions of the dynamics of reggezation of amplitudes in the quark-gluon picture. I express my gratitude for the hospitality at Jefferson Lab where this work was done.

## Appendix A. Relations between invariant and multipole amplitudes

In order to connect invariant and multipole amplitudes it is convenient to introduce the intermediate amplitudes  $f_i(s, \cos\theta, Q^2)$ :

$$f_1 = [(W - m_N)B_1 - B_5] \frac{[(E_1 + m_N)(E_2 + m_N)]^{1/2}}{8\pi W},$$

$$\begin{aligned}
f_2 &= -(W + m_N)B_1 - B_5 \frac{[(E_1 - m_N)(E_2 - m_N)]^{1/2}}{8\pi W}, \\
f_3 &= \left[ 2B_3 - B_2 + (W + m_N) \left( \frac{B_6}{2} - B_8 \right) \right] \frac{[(E_1 - m_N)(E_2 - m_N)]^{1/2} (E_2 + m)}{8\pi W}, \\
f_4 &= \left[ -(2B_3 - B_2) + (W - m_N) \left( \frac{B_6}{2} - B_8 \right) \right] \frac{[(E_1 + m_N)(E_2 + m_N)]^{1/2} (E_2 - m)}{8\pi W}, \\
f_5 &= \left\{ \left[ Q^2 B_1 + (W - m_N) B_5 + 2W(E_1 - m_N) \left( B_2 - \frac{W + m_N}{2} B_6 \right) \right] (E_1 + m_N) \right. \\
&\quad \left. - X \left[ (2B_3 - B_2) + (W + m_N) \left( \frac{B_6}{2} - B_8 \right) \right] \right\} \frac{(E_1 - m_N)(E_2 + m_N)}{8\pi W Q^2}, \\
f_6 &= \left\{ - \left[ Q^2 B_1 - (W + m_N) B_5 + 2W(E_1 + m_N) \left( B_2 + \frac{W - m_N}{2} B_6 \right) \right] (E_1 - m_N) \right. \\
&\quad \left. + X \left[ (2B_3 - B_2) - (W - m_N) \left( \frac{B_6}{2} - B_8 \right) \right] \right\} \frac{(E_1 + m_N)(E_2 - m_N)}{8\pi W Q^2},
\end{aligned} \tag{A.1}$$

where

$$X = \frac{\tilde{k}_0}{2}(t - m_\pi^2 + Q^2) - Q^2 \tilde{q}_0, \tag{A.2}$$

$\theta$  is the polar angle of the pion in the c.m.s.,  $\tilde{k}_0, \tilde{q}_0, E_1, E_2$  are the energies of virtual photon, pion, initial and final nucleons in this system.

The expansion of the intermediate amplitudes over multipole amplitudes  $M_{l\pm}(s, Q^2)$ ,  $E_{l\pm}(s, Q^2)$ ,  $S_{l\pm}(s, Q^2)$  has the form:

$$\begin{aligned}
f_1 &= \sum \left\{ (lM_{l+} + E_{l+})P'_{l+1}(\cos\theta) + [(l+1)M_{l-} + E_{l-}]P'_{l-1}(\cos\theta) \right\}, \\
f_2 &= \sum [(l+1)M_{l+} + lM_{l-}]P'_l(\cos\theta), \\
f_3 &= \sum \left[ (E_{l+} - M_{l+})P''_{l+1}(\cos\theta) + (E_{l-} + M_{l-})P''_{l-1}(\cos\theta) \right], \\
f_4 &= \sum (M_{l+} - E_{l+} - M_{l-} - E_{l-})P''_l(\cos\theta), \\
f_5 &= \sum \left[ (l+1)S_{l+}P'_{l+1}(\cos\theta) - lS_{l-}P'_{l-1}(\cos\theta) \right], \\
f_6 &= \sum [lS_{l-} - (l+1)S_{l+}]P'_l(\cos\theta).
\end{aligned} \tag{A.3}$$

The formulas which relate the amplitudes

$f_i(s, \cos\theta, Q^2)$  to the helicity amplitudes and cross section can be found in Ref. ([14]).

## Appendix B. Born contribution

The residues in the nucleon poles of the invariant amplitudes in Eqs. (3,4) are equal to:

$$\begin{aligned}
R_1^{(v,s)}(Q^2) &= \frac{ge}{2} \left( F_1^{(v,s)}(Q^2) + 2mF_2^{(v,s)}(Q^2) \right), \\
R_2^{(v,s)}(Q^2) &= -\frac{ge}{2} F_1^{(v,s)}(Q^2), \\
R_3^{(v,s)}(Q^2) &= -\frac{ge}{4} F_1^{(v,s)}(Q^2), \\
R_5^{(v,s)}(Q^2) &= \frac{ge}{4} (m_{\pi^2} - Q^2 - t) F_2^{(v,s)}(Q^2), \\
R_6^{(v,s)}(Q^2) &= ge F_2^{(v,s)}(Q^2), \\
R_8^{(v,s)}(Q^2) &= \frac{ge}{2} F_2^{(v,s)}(Q^2),
\end{aligned} \tag{B.1}$$

where  $g^2/4\pi = 14.2$ ,  $e^2/4\pi = 1/137$ , and  $F_1^{(v,s)}(Q^2)$ ,  $F_2^{(v,s)}(Q^2)$  are the nucleon Pauli form factors. Following Ref.[1], in the UIM the Lagrangian for the  $\pi NN$  vertex is taken in the form of mixed pseudovector (PV) and pseudoscalar (PS) couplings:

$$L_{\pi NN} = \frac{\Lambda^2}{\Lambda^2 + q^2} L_{\pi NN}^{PV} + \frac{q^2}{\Lambda^2 + q^2} L_{\pi NN}^{PS}, \tag{B.2}$$

where we take  $\Lambda^2 = 0.12 \text{ GeV}^2$ . This leads to the following additional contributions in the amplitudes  $B_1^{(+,0)}(s, t, Q^2)$ :

$$B_1^{(+,0)}(s, t, Q^2) = B_1^{(+,0)}(s, t, Q^2) + AF_2^{(v,s)}(Q^2), \tag{B.3}$$

where

$$A = \frac{ge}{2m_N} \frac{\Lambda^2}{\Lambda^2 + q^2}. \tag{B.4}$$

The nucleon Pauli form factors  $F_1^{(v,s)}(Q^2)$ ,  $F_2^{(v,s)}(Q^2)$  in the above equations we have defined according to the description of the existing data in Refs.[20, 21, 22] in the following way:

$$\begin{aligned}
F_1^{(v,s)}(Q^2) &= F_{1p}(Q^2) - F_{1n}(Q^2), \quad F_2^{(v,s)}(Q^2) = F_{2p}(Q^2) - F_{2n}(Q^2), \\
F_{1p}(Q^2) &= G_p^m(Q^2)/(1 + 2m_N z), \quad F_{2p}(Q^2) = z F_{1p}(Q^2), \\
z &= \frac{1.793}{2m_N} \left( 1 + \frac{1.2Q^2}{1 + 1.1Q} + 0.015Q^2 + 0.001Q^8 \right), \\
G_p^m(Q^2) &= 2.793/(1 + 0.35Q + 2.44Q^2 + 0.5Q^3 + 1.04Q^4 + 0.34Q^5),
\end{aligned} \tag{B.5}$$

$$\begin{aligned}
F_{1n}(Q^2) &= \frac{G_n^e(Q^2) + \tau G_n^m(Q^2)}{1 + \tau}, \quad F_{2n}(Q^2) = \frac{G_n^m(Q^2) - G_n^e(Q^2)}{2m_N(1 + \tau)}, \\
\tau &= Q^2/4m_N^2, \quad G_n^e = \frac{0.5Q^2}{1 + 25Q^4}, \quad G_n^m(Q^2) = -1.913F_d(Q^2), \\
F_d(Q^2) &= 1/(1 + 0.71/Q^2).
\end{aligned}$$

Here it is supposed that  $Q^2$  is taken in the  $GeV^2$  units. The pion form factor we take as in Ref. [1] in the form

$$F_\pi(Q^2) = F_1^{(v)}(Q^2). \quad (\text{B.6})$$

## Appendix C. Breit-Wigner parametrization for resonance contributions

We use the Breit-Wigner parametrization for the resonance contributions into multipole amplitudes in the form [7, 9]:

$$Res_{B-W}(W, Q^2) = c \left( \frac{k}{k_r} \right)^n \left( \frac{q_r}{q} \frac{k_r}{k} \frac{\Gamma_\pi \tilde{\Gamma}_\gamma}{\eta_\pi \Gamma} \right)^{1/2} \frac{M\Gamma}{M^2 - W^2 - iM\Gamma_{total}}, \quad (\text{C.1})$$

where  $n = 0$  for  $M_{l\pm}$ ,  $E_{l\pm}$ ,  $n = 1$  for  $S_{l\pm}$  and

$$\Gamma_{total} = \Gamma_\pi + \Gamma_{inel}, \quad (\text{C.2})$$

$$\Gamma_\pi = \eta_\pi \Gamma \left( \frac{q}{q_r} \right)^{2l+1} \left( \frac{X^2 + q_r^2}{X^2 + q^2} \right)^l, \quad (\text{C.3})$$

$$\tilde{\Gamma}_\gamma = \left( \frac{k}{k_r} \right)^{2l'+1} \left( \frac{X^2 + k_r^2}{X^2 + k^2} \right)^{l'}, \quad (\text{C.4})$$

$$\Gamma_{inel} = (1 - \eta_\pi) \Gamma \left( \frac{q_{2\pi}}{q_{2\pi,r}} \right)^{2l+4} \left( \frac{X^2 + q_{2\pi,r}^2}{X^2 + q_{2\pi}^2} \right)^{l+2}. \quad (\text{C.5})$$

For  $M_{l\pm}, E_{l\pm}, S_{l\pm}$   $l' = l$ , for  $E_{l-}, S_{l-}$   $l' = l - 2$  if  $l \geq 2$ , for  $S_{1-}$   $l' = 1$ ;  $M$  and  $\Gamma$  are masses and widths of the resonances,  $\eta_\pi$  are the branching ratios into the  $\pi N$  channel,  $q_{2\pi}$  is the 3-momentum of the  $2\pi$  system in the decay  $Resonance \rightarrow 2\pi + N$  in the c.m.s.,  $q_{2\pi,r}$  is the magnitude of this momentum at  $W = M$ ,  $X$  are phenomenological parameters.

For the resonance  $S_{11}(1535)$  which has large branching ratio into the  $\eta N$  channel,  $\Gamma_{total}$  is taken in the form

$$\Gamma_{total} = 0.6\Gamma_\pi + 0.1\Gamma_{inel} + 0.3\Gamma \frac{q_\eta}{q_\eta^r}. \quad (\text{C.6})$$

Below the thresholds of  $2\pi + N$  and  $\eta + N$  productions we take, respectively,  $q_{2\pi} = 0$  and  $q_\eta = 0$ .

## Appendix D. Invariant amplitudes in the Regge regime

In Ref. [10] the introduction of Regge-trajectories is made in gauge-invariant form for invariant amplitudes in the following way. Instead of t-channel  $\pi$  exchange, which is non-gauge-invariant and contributes into  $B_3^{(-)}(s, t, Q^2)$ , the following combination is used

$$\bar{u}(p_2)\gamma_5 \left\{ 2P^\mu B_2^{(-)} + 2q^\mu B_3^{(-)} \right\} u(p_1), \quad (\text{D.1})$$

where in addition to the  $\pi$  contribution, nucleon pole contribution generated by the form factor  $F_1^{(v)}(Q^2)$  is taken into account. The nucleon and pion contributions into  $B_2^{(-)}$  and  $B_3^{(-)}$  are written in the form:

$$B_2^{(-)}(s, t, q^2) = -\frac{ge}{2} F_1^{(v)}(Q^2) \left( \frac{t - m_\pi^2}{s - m^2} - \frac{t - m_\pi^2}{u - m^2} \right) \frac{1}{t - m_\pi^2}, \quad (\text{D.2})$$

$$B_3^{(-)}(s, t, q^2) = \left[ -\frac{ge}{4} F_1^{(v)}(Q^2) \left( \frac{t - m_\pi^2}{s - m^2} + \frac{t - m_\pi^2}{u - m^2} \right) - egF_\pi(Q^2) \right] \frac{1}{t - m_\pi^2}, \quad (\text{D.3})$$

and are reggeized by the replacement:

$$\frac{1}{t - m_\pi^2} \Rightarrow P_{Regge}^\pi \text{ in } B_{2,3}^{(-)} + P_{Regge}^{b_1} \text{ in } B_{2,3}^{(0)}. \quad (\text{D.4})$$

Here  $P_{Regge}$  are Regge propagators:

$$P_{Regge}^{\pi, b_1} = \left( \frac{s}{s_0} \right)^{\alpha_\pi(t)} \frac{\pi\alpha'_\pi}{\sin(\pi\alpha_\pi(t))} \frac{1}{\Gamma(1 + \alpha_\pi(t))} \frac{\tau + e^{-i\pi\alpha_\pi(t)}}{2}, \quad (\text{D.5})$$

and it is supposed that  $\pi$  and  $b_1$  trajectories are degenerate;  $\alpha_\pi(t) = \alpha'_\pi(t - m_\pi^2)$ ,  $\alpha'_\pi = 0.7 \text{ GeV}^2$ .

The contributions of the  $\rho$  and  $\omega$  exchanges in the  $t$ -channel are gauge invariant and are reggeized simply by the following replacements in Eqs. (E.1):

$$\frac{1}{t - m_\rho^2} \Rightarrow P_{Regge}^\rho \text{ in } B_i^{(0)} + P_{Regge}^{a_2} \text{ in } B_i^{(-)}, \quad i = 1, 2, 3, 6, \quad (\text{D.6})$$

$$\frac{1}{t - m_\omega^2} \Rightarrow P_{Regge}^\omega \text{ in } B_i^{(+)}, \quad i = 1, 2, 3, 6, \quad (\text{D.7})$$

where it is supposed that  $\rho$  and  $a_2$  trajectories are degenerate and

$$\begin{aligned} P_{Regge}^{\rho, a_2} &= \left(\frac{s}{s_0}\right)^{\alpha_\rho(t)-1} \frac{\pi\alpha'_\rho}{\sin(\pi\alpha_\rho(t)) \Gamma(\alpha_\rho(t))} \frac{1}{2} \frac{\tau + e^{-i\pi\alpha_\rho(t)}}{2}, \\ P_{Regge}^\omega &= \left(\frac{s}{s_0}\right)^{\alpha_\omega(t)-1} \frac{\pi\alpha'_\omega}{\sin(\pi\alpha_\omega(t)) \Gamma(\alpha_\omega(t))} \frac{1}{2} \frac{\tau + e^{-i\pi\alpha_\omega(t)}}{2}, \end{aligned} \quad (\text{D.8})$$

$\alpha_\rho(t) = 0.55 + \alpha'_\rho t$ ,  $\alpha'_\rho = 0.8 \text{ GeV}^2$ ,  $\alpha_\omega(t) = 0.44 + \alpha'_\omega t$ ,  $\alpha'_\omega = 0.9 \text{ GeV}^2$ . In Eqs. (D.5, D.8)  $\tau$  is the signature of the trajectory:

$$\tau_\pi = \tau_{a_2} = 1, \quad \tau_\rho = \tau_\omega = \tau_{b_1} = -1. \quad (\text{D.9})$$

## Appendix E. $\rho$ and $\omega$ contributions

The  $\rho$  and  $\omega$  exchanges in the  $t$  - channel contribute to the following amplitudes:

$$\begin{aligned} B_1^{(0)} &= \frac{e\lambda_\rho}{m_\pi} \left[ 2m_N g_{\rho 1} + t \frac{g_{\rho 2}}{2m_N} \right] \frac{1}{t - m_\rho^2}, \\ B_2^{(0)} &= \frac{e\lambda_\rho}{m_\pi} \frac{g_{\rho 2}}{4m_N} (Q^2 + m_\pi^2 - t) \frac{1}{t - m_\rho^2}, \\ B_3^{(0)} &= \frac{e\lambda_\rho}{m_\pi} \frac{g_{\rho 2}}{8m_N} (u - s) \frac{1}{t - m_\rho^2}, \quad B_6^{(0)} = 2 \frac{e\lambda_\rho}{m_\pi} g_{\rho 1} \frac{1}{t - m_\rho^2}, \\ B_1^{(+)} &= \frac{e\lambda_\omega}{m_\pi} \left[ 2m_N g_{\omega 1} + t \frac{g_{\omega 2}}{2m_N} \right] \frac{1}{t - m_\omega^2}, \\ B_2^{(+)} &= \frac{e\lambda_\omega}{m_\pi} \frac{g_{\omega 2}}{4m_N} (Q^2 + m_\pi^2 - t) \frac{1}{t - m_\omega^2}, \\ B_3^{(+)} &= \frac{e\lambda_\omega}{m_\pi} \frac{g_{\omega 2}}{8m_N} (u - s) \frac{1}{t - m_\omega^2}, \quad B_6^{(+)} = 2 \frac{e\lambda_\omega}{m_\pi} g_{\omega 1} \frac{1}{t - m_\omega^2}. \end{aligned} \quad (\text{E.1})$$

These amplitudes are obtained using vertexes  $\gamma\rho\pi$ ,  $\gamma\omega\pi$ ,  $\rho NN$  and  $\omega NN$  defined in the form presented in Ref. [1]. In the UIM, the off-shell behaviour of  $g_{Vi}$  is described by:  $g_{Vi} = \tilde{g}_{Vi}\Lambda_V^2/(\Lambda_V^2 - t)$ . The coupling constants are taken from Ref. [1] and are equal to:

$$\begin{aligned}\lambda_\omega &= 0.314, \quad \tilde{g}_{\omega 1} = 21, \quad \tilde{g}_{\omega 2} = -12, \quad \Lambda_\omega = 1.2, \\ \lambda_\rho &= 0.103, \quad \tilde{g}_{\rho 1} = 2, \quad \tilde{g}_{\rho 2} = 13, \quad \Lambda_\rho = 1.5.\end{aligned}\quad (\text{E.2})$$

In the Regge-pole analysis of high energy photoproduction data in Ref. [10] the coupling constants are:

$$g_{\omega 1}^{Regge} = 13.9, \quad g_{\omega 2}^{Regge} = 0, \quad g_{\rho 1}^{Regge} = 3.47, \quad g_{\rho 2}^{Regge} = 13. \quad (\text{E.3})$$

## References

- [1] D.Drechsel, O.Hanstein, S.S.Kamalov, L.Tiator, Nucl.Phys. **A645**, 145 (1999).
- [2] R.A.Arndt, I.I.Strakovsky, R.L.Workman, Phys.Rev. **C53**, 430 (1996).
- [3] R.A.Arndt, W.J.Briscoe, I.I.Strakovsky, R.L.Workman, e-print nucl-th/0205067.
- [4] S.Weinberg, Phys. Rev. Let. **18**, 188 (1967); Phys.Rev. **166**, 1568 (1968).
- [5] R.D.Peccei, Phys.Rev. **181**, 1902 (1969).
- [6] R.M.Davidson, N.C.Mukhopadhyay, R.S.Witman, Phys. Rev. **D43**, 71 (1991).
- [7] R.L.Walker, Phys. Rev. **182**, 1729 (1969).
- [8] K.M.Watson, Phys. Rev. **95**, 228 (1954).
- [9] R.C.E.Devenish, D.H.Lyth, Phys. Rev. **D5**, 47 (1972).

- [10] M.Gidal, J.-M.Laget, M.Vanderhaegen, Nucl. Phys. **A627**, 645 (1997); Phys. Lett. **B400**, 6 (1997).
- [11] R.A.Arndt, I.I.Strakovsky, R.L.Workman, M.M.Pavan, Phys.Rev. **C52**, 2120 (1995).
- [12] D.Schwela, H.Rolnik, R.Weizel, W.Korth, Z. Phys. **202**, 452 (1967).
- [13] D.Schwela, R.Weizel, Z. Phys. **221**, 71 (1969).
- [14] I.G.Aznauryan, Phys. Rev. **D57**, 2727 (1998).
- [15] R.C.E.Devenish, D.H.Lyth, Nucl. Phys. **B93**, 109 (1975).
- [16] S.S.Kamalov et al., Phys. Rev. **C64**, 033201 (2001).
- [17] R.A.Arndt et al., Phys.Rev. **D43**, 2131 (1991).
- [18] V.V.Frolov et al., Phys. Rev. Let. **82**, 45 (1999).
- [19] K.Joo et al., Phys. Rev. Let. **88**, 122001 (2002).
- [20] M.K.Jones et al., Phys. Rev. Let. **84**, 1398 (2000).
- [21] Kees de Jager, JLAB preprint JLAB-PHY-00-01.
- [22] P.Bosted et al., Phys. Rev. **C51**, 718 (1995).

## Figure Captions

**Fig. 1.** (a) Multipole amplitude  $M_{1+}^{3/2}$  within DR. The results are obtained via solution of the integral equation (8): solid and dashed curves correspond to the real and imaginary parts of the amplitude, dotted and dashed-dotted curves correspond to the contributions of homogeneous and particular solutions into  $ImM_{1+}^{3/2}$ , thin dashed curve is the contribution of other multipoles into (8).

(b) Multipole amplitude  $E_{1+}^{3/2}$  within DR and UIM. Dashed-dotted and dashed curves are the real and imaginary parts of the amplitude obtained by DR via solution of the integral equation (8), thin dashed curve is the contribution of other multipoles into (8); solid and dotted curves are the real and imaginary parts of the amplitude obtained within UIM with modified background, thin solid curve is obtained with the background of Ref. [1].  
(c)  $ImM_{1+}^{3/2}$  in the UIM: solid curve is the full result obtained with the modified background, dashed-dotted and dashed curves correspond to the resonance and background contributions, respectively, dotted curve is the background of the UIM of Ref. [1].

(d)  $ReM_{1+}^{3/2}$  in the UIM: the legend is as for Fig. 1c.

In Figs. 1a-d, the GWU(VPI) results from the SAID program are presented by open circles for the imaginary parts of the amplitudes and by solid triangles for those real parts.

**Fig. 2.** Multipole amplitudes within DR and UIM. Dashed-dotted and dashed curves are the real and imaginary parts of amplitudes obtained by DR. Solid and dotted curves are the real and imaginary parts of amplitudes obtained within UIM with modified background, thin solid curves are obtained with the background of Ref. [1]. Plotted are the multipole amplitudes in millifermi units, in the parentheses the notations of multipole amplitudes in SAID program are given. The GWU(VPI) results from the SAID program are presented by open circles for the real parts of the amplitudes and by solid triangles for those imaginary parts.

**Fig. 3.** The contributions of the integral over  $M_{1+}^{3/2}$  (in millifermi units) into the real

parts of the multipole amplitudes  $E_{0+}^{\frac{1}{2}}$  (dashed curve),  $E_{0+}^{\frac{3}{2}}$  (dashed-dotted curve),  $M_{1-}^{\frac{1}{2}}$  (solid curve),  $M_{1-}^{\frac{3}{2}}$  (dotted curve) within dispersion relations.

**Fig. 4.** The imaginary part of  $M_{1+}^{\frac{3}{2}}$  obtained within DR (dashed curves) and UIM (solid curves) at  $Q^2 = 0, 0.9, 1.8, 2.8, 4 \text{ GeV}^2$ . Data at  $Q^2 = 0$  are from GWU(VPI) analysis, data at other  $Q^2$  are the same data with changed normalizations.

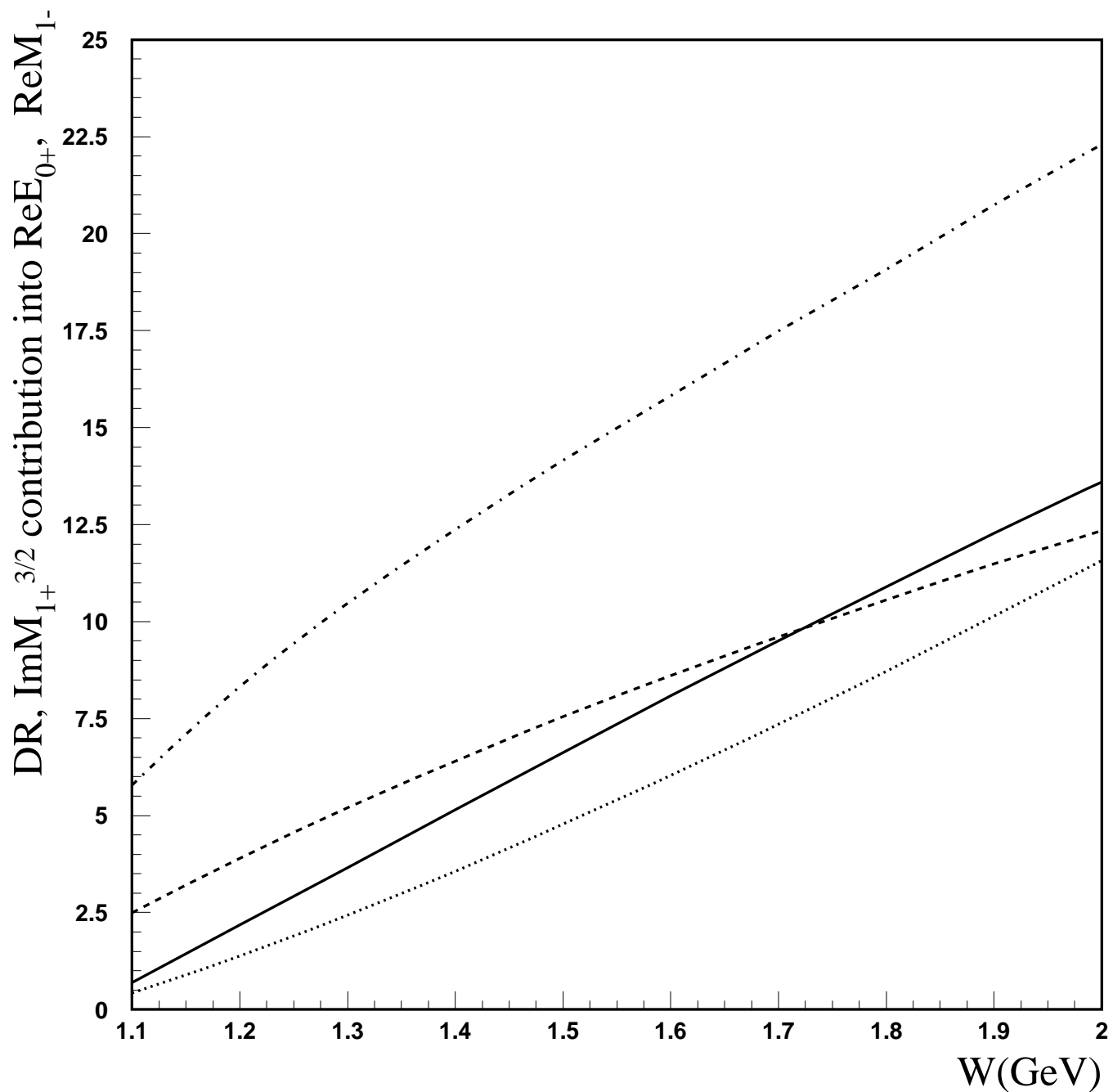


**Fig. 3**

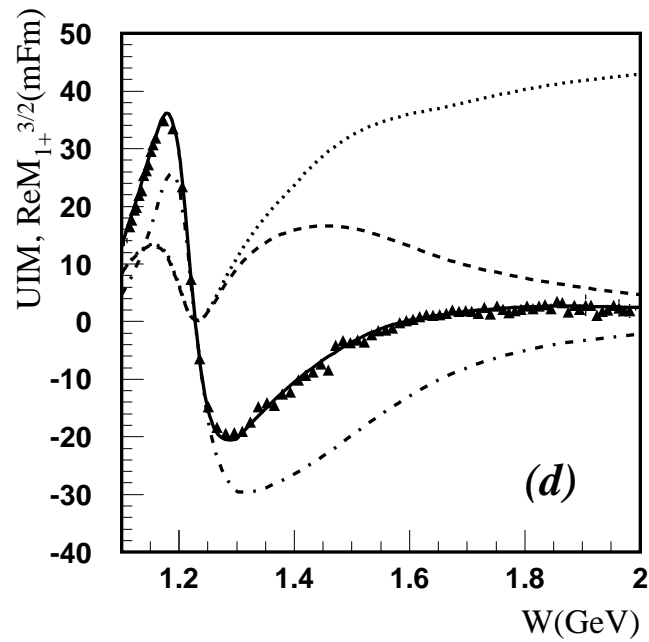
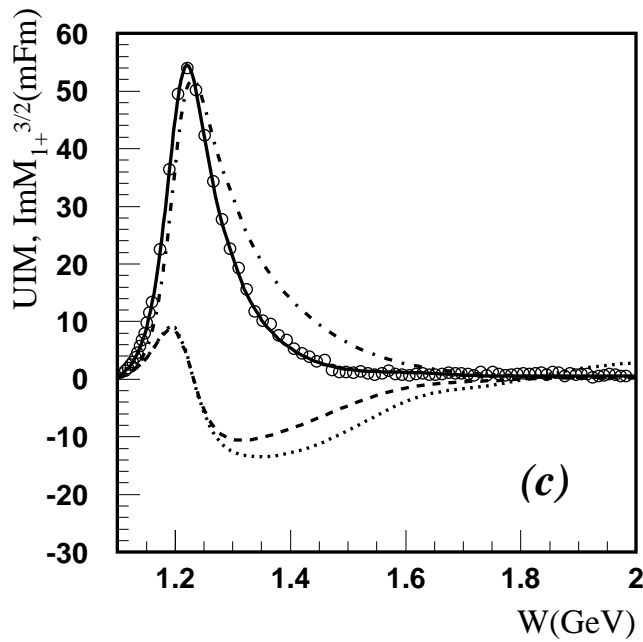
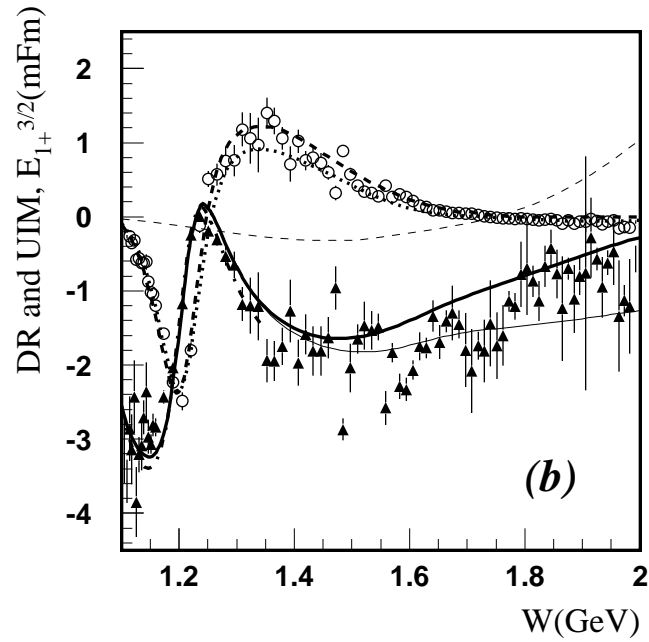
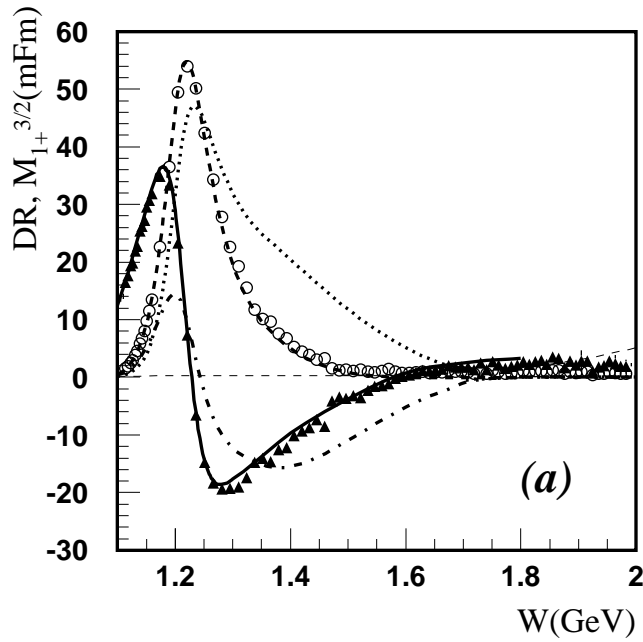
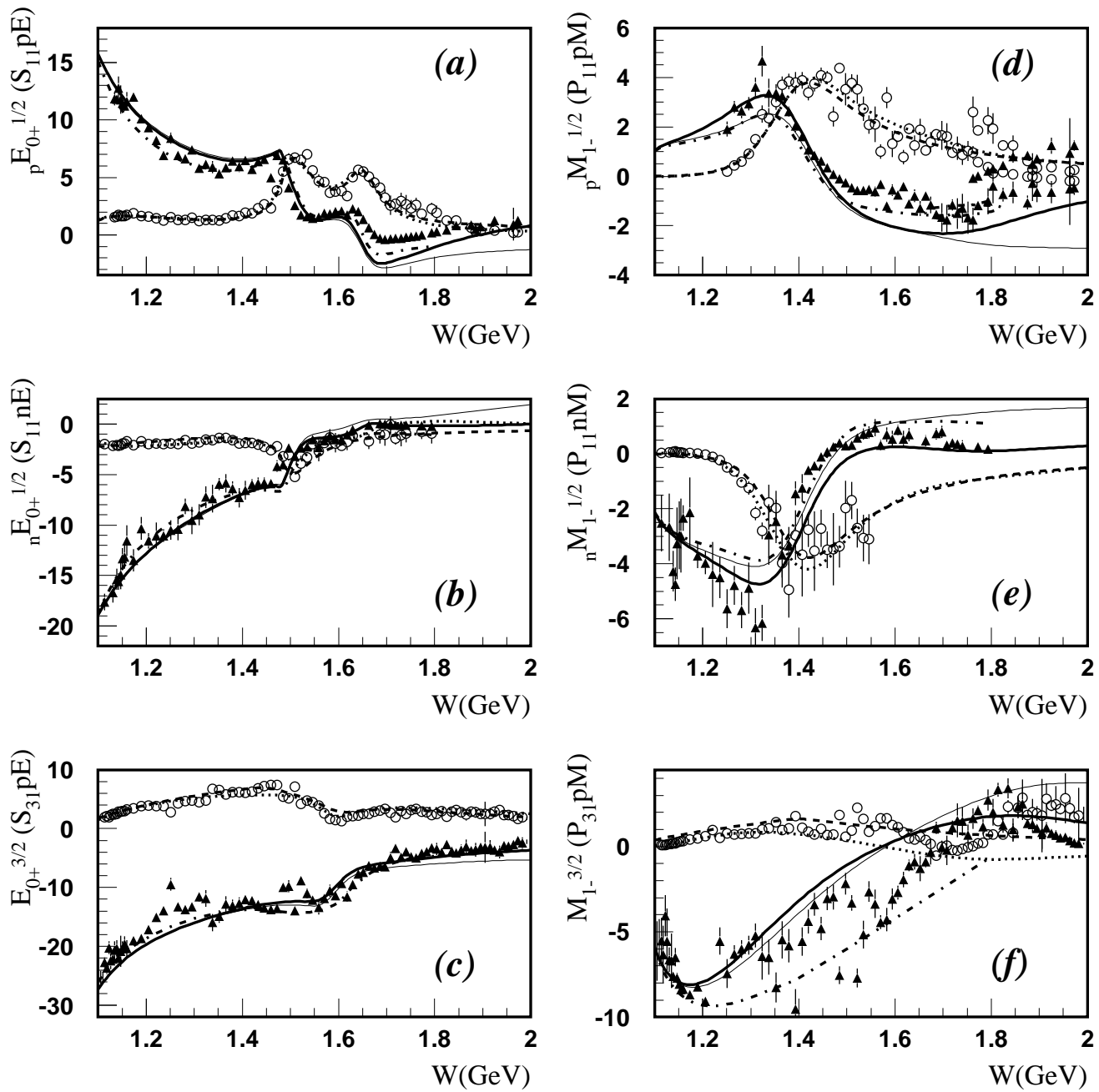


Fig. 1



**Fig. 2**

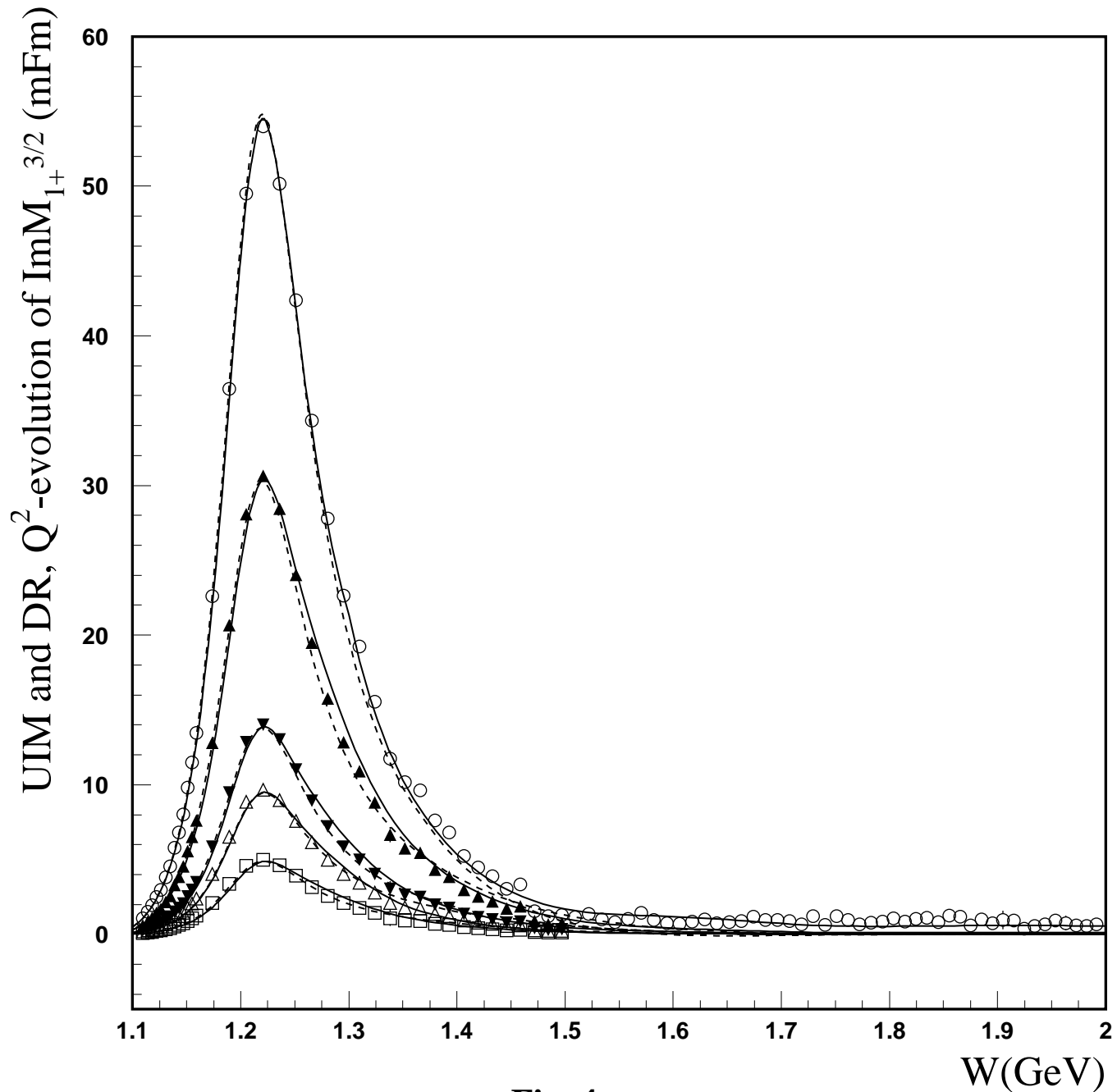
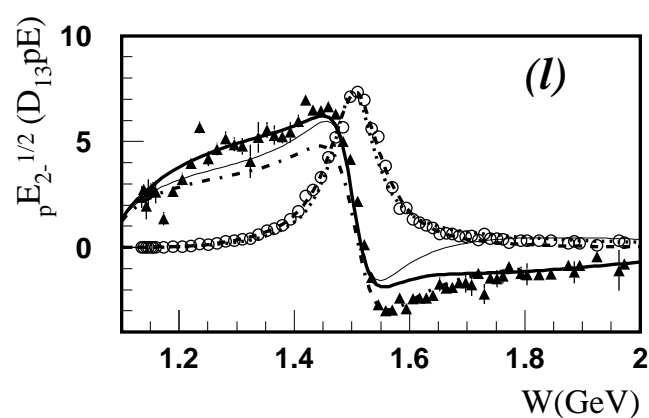
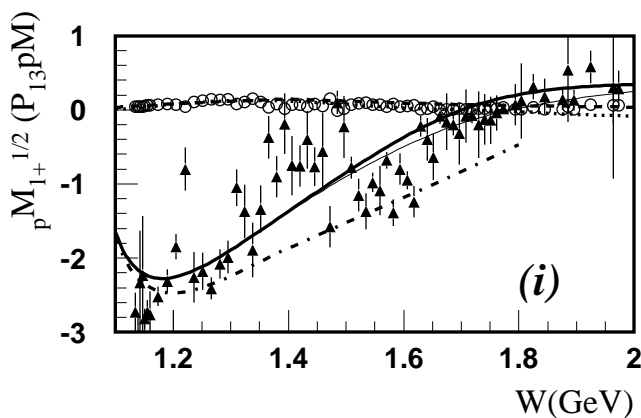
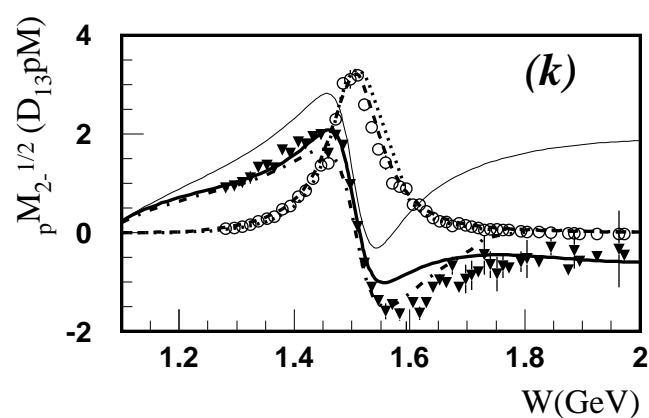
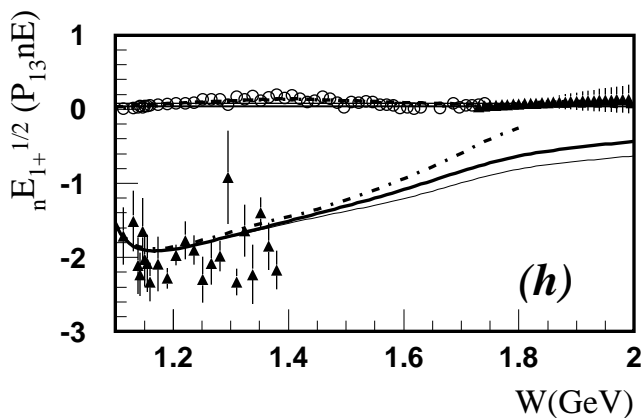
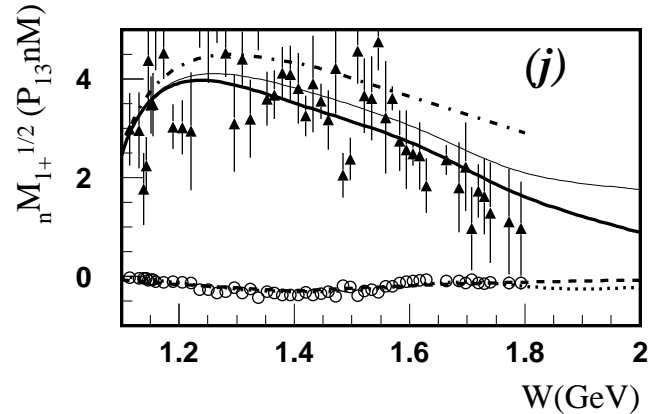
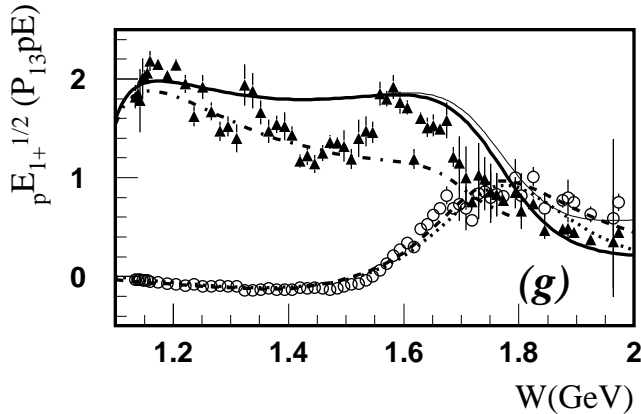
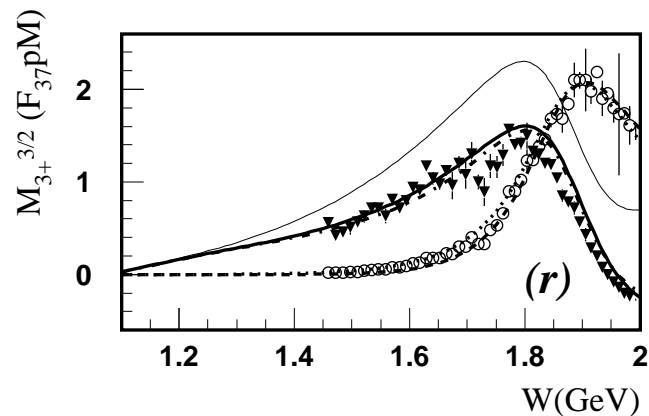
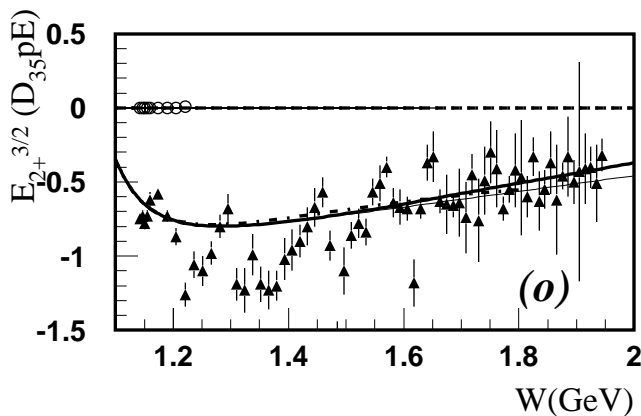
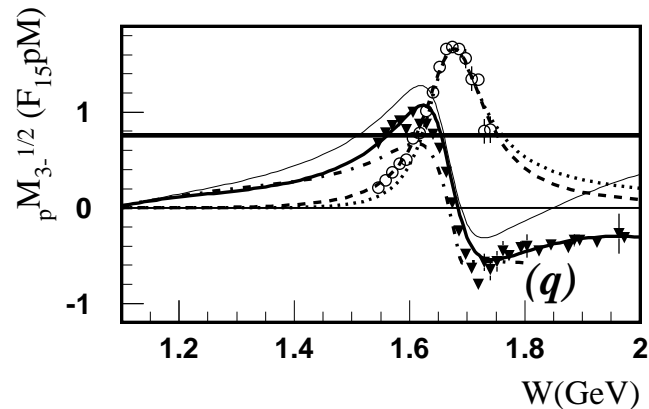
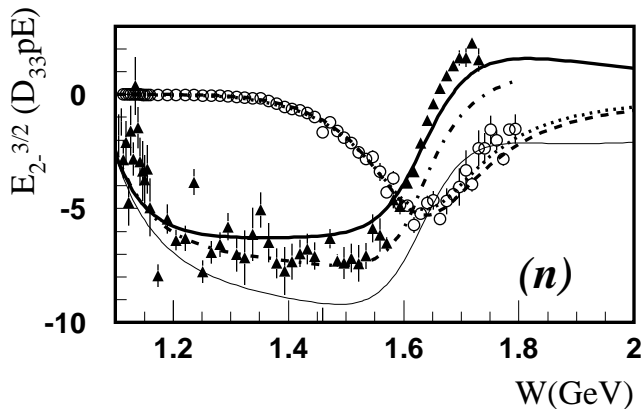
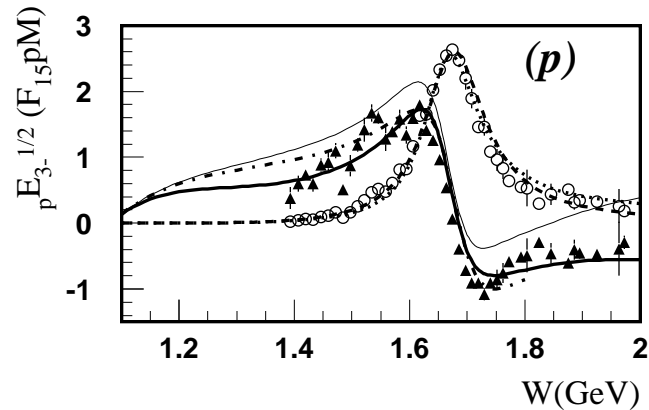
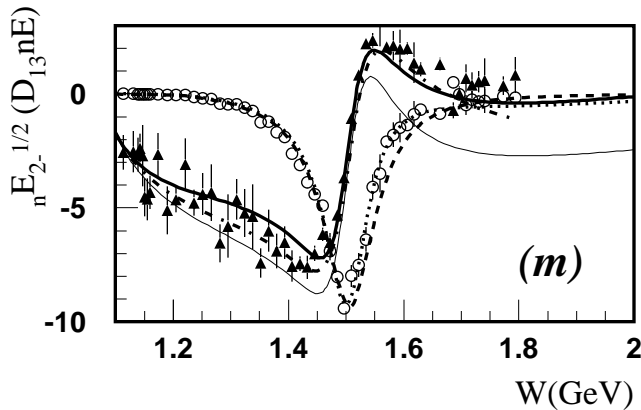


Fig. 4



**Fig. 2 (continued)**



**Fig. 2 (continued)**